IAI Journals.ASM.org

Thiol Peroxidase Is an Important Component of *Streptococcus pneumoniae* in Oxygenated Environments

Barak Hajaj,[a] Hasan Yesilkaya,[b] Rachel Benisty,[a] Maayan David,[a] Peter W. Andrew,[b] and Nurith Porat[a]

Pediatric Infectious Disease Unit, Soroka University Medical Center, Faculty of Health Sciences, Department of Microbiology and Immunology, Ben-Gurion University of the Negev, Beer Sheva, Israel,[a] and Department of Infection, Immunity and Inflammation, University of Leicester, Leicester, United Kingdom[b]

***Streptococcus pneumoniae* is an aerotolerant Gram-positive bacterium that causes an array of diseases, including pneumonia, otitis media, and meningitis. During aerobic growth, *S. pneumoniae* produces high levels of H_2O_2. Since *S. pneumoniae* lacks catalase, the question of how it controls H_2O_2 levels is of critical importance. The *psa* locus encodes an ABC Mn^{2+}-permease complex (*psaBCA*) and a putative thiol peroxidase, *tpxD*. This study shows that *tpxD* encodes a functional thiol peroxidase involved in the adjustment of H_2O_2 homeostasis in the cell. Kinetic experiments showed that recombinant TpxD removed H_2O_2 efficiently. However, *in vivo* experiments revealed that TpxD detoxifies only a fraction of the H_2O_2 generated by the pneumococcus. Mass spectrometry analysis demonstrated that TpxD Cys^{58} undergoes selective oxidation *in vivo*, under conditions where H_2O_2 is formed, confirming the thiol peroxidase activity. Levels of TpxD expression and synthesis *in vitro* were significantly increased in cells grown under aerobic versus anaerobic conditions. The challenge with D39 and TIGR4 with H_2O_2 resulted in *tpxD* upregulation, while *psaBCA* expression was oppositely affected. However, the challenge of Δ*tpxD* mutants with H_2O_2 did not affect *psaBCA*, implying that TpxD is involved in the regulation of the *psa* operon, in addition to its scavenging activity. Virulence studies demonstrated a notable difference in the survival time of mice infected intranasally with D39 compared to that of mice infected intranasally with D39Δ*tpxD*. However, when bacteria were administered directly into the blood, this difference disappeared. The findings of this study suggest that TpxD constitutes a component of the organism's fundamental strategy to fine-tune cellular processes in response to H_2O_2.**

Streptococcus pneumoniae is an aerotolerant, Gram-positive bacterium that causes an array of diseases, including pneumonia, otitis media, and meningitis (18). The pneumococcus is exposed to different levels of oxygen during infection; for example, in the nasopharynx and lungs, it is exposed to a partial pressure of oxygen close to that of the atmosphere, while the blood is much less oxygenated (3). During aerobic growth, *S. pneumoniae* produces exceptionally high levels of H_2O_2 (up to 1 mM), mediated mainly by pyruvate oxidase (34). Although H_2O_2 serves as an intracellular messenger at low concentrations, it induces cell death at higher concentrations (44). Furthermore, the reactive oxygen species produced by host immune cells also pose a threat for the pneumococcus and, hence, must be adequately detoxified (35, 43). Since *S. pneumoniae* lacks catalase, the question of how it defends itself against hazardous levels of H_2O_2 is of critical importance.

Certain aspects of the pneumococcal response to oxidative stress have been described, but the overall data are incomplete. The activities of some key enzymes involved in the oxidative stress response, including superoxide dismutase (45), NADH oxidase (3), and alkyl hydroperoxidase (32), and their contribution to *S. pneumoniae* survival (3, 45) have already been described. Additionally, some of the pneumococcal surface antigens were also linked to the oxidative stress response, such as pneumococcal surface antigen A (PsaA) and pneumococcal surface antigen D (PsaD) (also known as Tpx, because it is believed to be a thiol peroxidase) (27, 42). The inactivation of these proteins renders pneumococci susceptible to oxidative stress.

The *psa* locus of *S. pneumoniae* encodes an ABC Mn^{2+}-permease complex (*psaBCA*) immediately upstream of *psaD* (*tpxD*) coding for the putative thiol peroxidase (29). Although the involvement of *tpxD* in the pneumococcal oxidative stress response has been shown, the data have been scant (26, 42). The *tpxD* gene encodes a protein of 163 amino acid residues, which shares 53% and 46% identities with the Tpx proteins of *Bacillus subtilis* and *Escherichia coli*, respectively (22, 29). The quaternary structure of the putative *S. pneumoniae* TpxD protein was reported previously (PDB accession number 1PSQ) (39). The sequence alignment and structural superposition of TpxD with Tpx proteins from other bacterial species suggested that Cys^{58} is the conserved peroxidatic cysteine that is oxidized to cysteine sulfenic acid (Cys-SOH) by peroxides during the catalytic cycle and that Cys^{92} is the resolving cysteine that attacks Cys-SOH and forms an intramolecular disulfide bond. It would be expected that the catalytic cycle is completed with the reduction of the disulfide bond by a cell-specific oxidoreductase, e.g., thioredoxin (39). The redox states of the two TpxD cysteines have not been demonstrated *in vivo*. The present study establishes that pneumococcal *tpxD* encodes a functional thiol peroxidase and that TpxD plays a role in the precise control of H_2O_2 levels. Moreover, our data show for the first time that TpxD is involved in the regulation of the *psaBCA* genes. By using

Received 6 February 2012 **Returned for modification** 21 March 2012
Accepted 21 September 2012
Published ahead of print 1 October 2012
Editor: J. N. Weiser
Address correspondence to Nurith Porat, npurat@bgu.ac.il.
B.H. and H.Y. contributed equally to this work. N.P. and P.W.A. contributed equally to this work.
Supplemental material for this article may be found at http://iai.asm.org/.

doi:10.1128/IAI.00126-12

a thiol-trapping method and mass spectrometry (MS), we show that Cys^{58} of TpxD undergoes selective oxidation under conditions where H_2O_2 is formed. In addition, TpxD expression is modulated, both *in vivo* and *in vitro*, in accordance with H_2O_2 levels, reinforcing the conclusion that it has a role in maintaining homeostatic peroxide levels in *S. pneumoniae*.

MATERIALS AND METHODS

Bacterial growth conditions. *Streptococcus pneumoniae* D39 (serotype 2) and TIGR4 (serotype 4) were used in this study. Routinely, pneumococci were grown at 37°C in brain heart infusion (BHI) broth or Todd-Hewitt (TH) broth with 0.5% (wt/vol) yeast extract (THY) to an optical density at 620 nm (OD_{620}) of 0.25 to 0.3 or on blood agar plates supplemented with 5% (vol/vol) defibrinated sheep blood under microaerophilic conditions at 37°C. Bacteria (200 ml) were grown in 500-ml aerated bottles in a shaking water bath (130 rpm) for aerobic conditions or in closed, completely filled 20-ml test tubes in a water bath without shaking for anaerobic conditions. The D39 and TIGR4 *tpxD* mutants (D39Δ*tpxD* and TIGR4Δ*tpxD*) were grown in medium supplemented with 100 μg/ml spectinomycin, and the D39Δ*tpxD*-complemented strain (D39Δ*tpxD*comp) was grown in medium supplemented with 100 μg/ml spectinomycin and 500 μg/ml kanamycin.

Construction of the *tpxD* mutant in D39 and TIGR4. To construct the Δ*tpxD* mutant, a 1,768-bp genomic region containing *tpxD* (SPD1464) was amplified from D39 DNA with primers SPD1464F (GCTTGGCTTAACCTTGAAAAC) and SPD1464R (GCCAACACTTATCTGGTCTC). The amplicons were incubated with the *Himar1* transposase (19) and plasmid pR412, which contains the *mariner* minitransposon conferring spectinomycin resistance (25). The *in vitro*-mutagenized DNA was then transformed into D39 and TIGR4 cells by using competence-stimulating peptide (1). Transformants were selected for spectinomycin resistance, and the insertion of the resistance cassette was confirmed by PCR using transposon-specific primer MP127 or MP128, with appropriate chromosomal primers, and sequenced as described previously (47). The transformants were selected on blood agar plates supplemented with spectinomycin (100 μg/ml). Representative D39Δ*tpxD* and TIGR4Δ*tpxD* strains were selected for further analysis.

Complementation of D39Δ*tpxD*. To eliminate the possibility of polar effects from the *tpxD* mutation, *tpxD* was complemented with an intact copy of the gene by using pCEP, which is a nonreplicative plasmid that allows controlled gene expression following ectopic integration into the chromosome (11). The entire *tpxD* sequence, as well as 83 bp upstream of the gene, was amplified with primers tpxDNcoI (CG*CCATGG*CGTCATTCTCATGTGAGCTGGC) and tpxDBamHI (ACG*GGATCC*CCTATAGGGCTTTAGCAGCTGCA), which introduced NcoI and BamHI sites (italicized) into the 5′ and 3′ ends of the amplicons, respectively. After the amplicons were digested with NcoI and BamHI, they were purified and ligated into the NcoI- and BamHI-digested vector. An aliquot of the ligation mixture was transformed into Stellar competent cells (Clontech, Saint-Germain-en-Laye, France) according to the manufacturer's instructions. The transformants were selected on kanamycin-containing (500 μg/ml) Luria-Bertani (LB) medium agar plates. Colony PCR for selected transformants with primers MalF (GCTTGAAAAGGAGTATACTT) and pCEPR (AGGAGACATTCCTTCCGTATC), whose recognition sites are localized immediately up- and downstream of the cloning site, respectively, and amplify an approximately 263-bp product in the empty vector, produced an approximately 755-bp product (data not shown), indicating that successful cloning had taken place (the additional 492 bp represents the cloned fragment containing *tpxD*). The recombinant plasmid was purified by using a commercial kit (Qiagen), and an aliquot was transformed into D39Δ*tpxD* cells as described previously (1). The transformants were selected on blood agar plates supplemented with spectinomycin (100 μg/ml) and kanamycin (500 μg/ml).

Expression and purification of TpxD. The coding sequence of *tpxD* was amplified by PCR from a single colony of *S. pneumoniae* D39 and subcloned into the pRSETc vector (Invitrogen) between the XhoI and KpnI sites. *Escherichia coli* BL21 cells harboring the constructed plasmid were grown in LB medium supplemented with ampicillin (100 μg/ml) for 24 h. Cells were harvested by centrifugation and stored at −70°C. The pellet was suspended in lysis buffer (50 mM Tris [pH 8], 100 mM phenylmethylsulfonyl fluoride [PMSF]), disintegrated by sonication, and centrifuged at 4,000 × *g* for 1 h. Proteins in the supernatant were loaded onto a Ni-nitrilotriacetic acid (NTA) column (Adar Biotec, Israel) and incubated for 1 h at 4°C. The column was then washed with 10 mM imidazole, and the recombinant protein was eluted from the column with 100 mM imidazole. SDS-PAGE of purified TpxD gave one band, which was of the predicted molecular mass (data not shown).

Immunization of rabbits. Three-month-old albino rabbits (Harlan Laboratories, Israel) were immunized subcutaneously with 100 to 200 μg of purified TpxD (extracted from SDS-PAGE gels) in complete Freund's adjuvant. Booster immunizations with the same dose were performed with incomplete Freund's adjuvant. Antisera were collected 3 weeks after the last immunization.

SDS-PAGE and Western blotting. Pneumococci were lysed and subjected to SDS-PAGE. Separated proteins were electroblotted onto a 0.45-μm nitrocellulose membrane (Bio-Rad, CA) and probed with the polyclonal rabbit anti-TpxD serum. Antigen complexes were detected by using Peroxidase Affinity Pure goat anti-rabbit IgG (Jackson ImmunoResearch, PA) and visualized with SuperSignal West Pico chemiluminescent substrate (Pierce, IL).

NADPH-linked peroxidase activity assays. The peroxidase activity of recombinant TpxD was determined according to methods described previously by Atack et al. (2), with some modifications. Briefly, pure thioredoxin (Trx) and thioredoxin reductase (TrxR) from *E. coli* were obtained from Sigma-Aldrich (United Kingdom). The reaction mixture contained 100 mM HEPES-NaOH (pH 7.0), 200 μM NADPH, 3,420 μM Trx, 360 μM TrxR, 5 μM TpxD, and various hydrogen peroxide concentrations (0.25 μM to 50 mM). Reactions were carried out with a total volume of 200 μl at 25°C and were started by the addition of H_2O_2 to the mixture. The decrease in the NADPH absorbance was monitored at 340 nm with a μQuant spectrophotometer (Bio-tek Instruments). In control experiments, thioredoxin, thioredoxin reductase, TpxD, or H_2O_2 was omitted from the reaction mixtures. Constants were calculated by using GraphPad Prism 5 software (GraphPad Software Inc., San Diego, CA).

Determination of the TpxD cysteine-thiol redox state by trapping with AMS. D39 cells were grown under aerobic conditions to an OD_{620} of 0.25. Alkylation was performed as previously described (7). Briefly, protein-thiols in the reduced state were blocked by resuspending bacteria washed with phosphate-buffered saline (PBS) in 100 μl ice-cold AMS buffer (0.1 M Tris [pH 8], 1 mM EDTA, 1% [wt/vol] SDS) supplemented with 20 mM 4-acetamido-4′-maleimidylstilbene-2,2′-disulfonic acid (AMS; Invitrogen) and sonicated for 10 s. Alkylation was performed at room temperature for 2 h and stopped by the addition of a one-quarter volume of nonreducing sample buffer (0.1 M Tris [pH 6.8], 25 mM EDTA, 5% [wt/vol] SDS, 20% [vol/vol] glycerol) to the mixture. When indicated, dithiothreitol (DTT) treatment was done by incubating lysates of aerobically grown bacteria with 50 mM DTT at 37°C for 30 min prior to AMS alkylation. Following alkylation, samples (2×10^8 CFU) were loaded onto 18% (wt/vol) polyacrylamide–SDS gels and immunoblotted by using TpxD polyclonal antibodies. Densitometry was performed by using Gel-Quant image analysis software (AMPL Software).

Determination of the TpxD cysteine-thiol redox state by mass spectrometry. D39 cells were grown under aerobic conditions to an OD_{620} of 0.25. Alkylation was performed as previously described (9). Briefly, protein-thiols in the reduced state from DTT-treated (40 mM) and untreated D39 cells were blocked by resuspending bacteria washed in PBS in urea buffer (0.1 M Tris [pH 8.2], 1 mM EDTA, 8 M urea) containing 110 mM iodoacetic acid (IAA). Following alkylation, samples (2.6×10^8 CFU) were resolved on 18% (wt/vol) SDS-PAGE gels and stained with Coomassie blue, and a band corresponding to ~18 kDa was cut from the gel, reduced with 2.8 mM DTT (60°C for 30 min), and modified with 8.8 mM

iodoacetamide (IAM) in 100 mM ammonium bicarbonate (in the dark at room temperature for 30 min). The modified protein was then digested with chymotrypsin (Promega) in 10% (vol/vol) acetonitrile and 10 mM ammonium bicarbonate overnight at 37°C. The resulting peptides were resolved by reverse-phase chromatography on 0.075- by 200-mm fused silica capillaries (J&W) packed with Reprosil reversed-phase material (Dr. Maisch GmbH, Germany). Mass spectrometry was performed with an ion-trap mass spectrometer (Orbitrap; Thermo Scientific) in a positive mode using a repetitively full MS scan followed by the collision-induced dissociation of the 7 most dominant ions selected from the first MS scan. The mass spectrometry data were clustered and analyzed by using Sequest software (J. Eng and J. Yates, University of Washington, and Finnigan, San Jose, CA) and Pep-Miner (6), searching against the *S. pneumoniae* database.

H_2O_2 survival assay. D39 and D39Δ*tpxD* cells grown under aerobic conditions to an OD_{620} of 0.3 were incubated with 40 mM or 20 mM H_2O_2 (Sigma) at 37°C for 15 min. Serial dilutions were spotted onto 5% (vol/vol) blood agar plates. The percent survival was calculated by dividing the CFU of cultures after exposure to H_2O_2 by the CFU in the control culture without H_2O_2. Chain formation by H_2O_2-treated and untreated bacteria was viewed by using an Olympus BX41 microscope fitted with an Olympus DP72 camera and Cellesense Entry software (MATIMOP, Israel).

Measurement of H_2O_2 levels. Hydrogen peroxide production was analyzed by a spectrophotometric assay adapted from a method described previously by Pericone et al. (33), with some modifications. Briefly, 2.8×10^8 pneumococci in 2.5 ml medium were centrifuged at 4°C for 20 min at 4,000 × *g*, washed with ice-cold PBS (pH 7.2), and resuspended in 5 ml PBS containing 0.5 mM glucose. After 1 h of incubation at 37°C, supernatants were diluted with 1× reaction buffer of the Amplex Red H_2O_2 assay kit (Molecular Probes), and H_2O_2 levels were measured according to the manufacturer's instructions.

RNA extraction from *in vitro*-grown bacteria. RNA from *in vitro*-grown bacteria was prepared as previously described (7).

RNA quantitation by real-time reverse transcription (RT)-PCR. cDNA was synthesized with a Verso cDNA kit (ABgene, United Kingdom). PCR mixtures contained Absolute blue QPCR SYBR mix ROX (ABgene, United Kingdom) and the following primers (designed with Primer Express Software, version 3.0 [Applied Biosystems, United Kingdom]): tpxF (5′-AGAATTGGCTGGACTGGACAA-3′) and tpxR (5′-CACCGCACCAACGTTTTTG-3′) for *tpxD*, psaAF (5′-ACTCATTGTAACCAGCGAAGGAGCA-3′) and psaAR (5′-CCCAGATGTAGGCACTTGGAACACC) for *psaA*, psaBF (5′-TCAAGGTCAAGGAATGCGTCTCGT-3′) and psaBR (5′-AGTCAGCTAGGCCGACGATTTCAA) for *psaB*, and PsaCF (5′-ATTGTAGCTGGAGCTGTGGGATGT-3′) and psaCR (5′-AGCAATCCAAAGACAATGGCTCCG-3′) for *psaC*. The transcription level was normalized to the level of the *gyrA* gene, which was amplified with primers gyrAF (5′-CGTAGAGAATGCGACGGTGAA-3′) and gyrAR (5′-GTTATCGTAGCGCGAGCTCTTC-3′). The results were analyzed by the comparative threshold cycle (C_T) method (21).

***In vivo* virulence studies.** Ten-week-old female MF1 outbred mice (Charles River, Margate, United Kingdom) were used for virulence testing. A standardized inoculum was prepared as described previously (45–47). To determine the virulence of pneumococcal strains, mice were lightly anesthetized with 3% (vol/vol) isoflurane over oxygen, and a 50-μl sample of PBS containing approximately 1×10^6 CFU was given dropwise into the nostrils. The inoculum dose was confirmed by viable counting on blood agar plates. Mice were monitored for disease signs (progressively starry coat, hunched, and lethargic) for 7 days (28), and those that reached the severely lethargic stage were considered to have reached the endpoint of the assay and were killed humanely. The time to this point was defined as the "survival time." Mice that were alive 7 days after infection were deemed to have survived the infection. For intravenous infections, approximately 5×10^5 CFU of *S. pneumoniae* in 100 μl PBS (pH 7.0) were administered via the dorsal tail vein. The inoculum dose was confirmed by plating onto blood agar, as described above. Survival times were calculated by using GraphPad Prism software and analyzed by the Mann-Whitney U test. Statistical significance was considered to be a P value of <0.05.

To determine the development of bacteremia in each mouse, approximately 20 μl of venous blood was obtained from intranasally infected mice at predetermined time points after infection, and viable counts were determined, as described above.

The growth of pneumococci in the nasopharynx was also determined, as described previously (41). For this, at predetermined time intervals following intranasal infection, set groups of mice were deeply anesthetized with 5% (vol/vol) isoflurane over oxygen, and the mice were subsequently killed by cervical dislocation. Mice were pinned onto a dissection board face up, and the mandible was removed. After introducing two lateral incisions (left and right) starting from the soft palate toward the pane, the palate was pulled back by forceps. The exposed nasopharyngeal tissue was collected, transferred into 10 ml of sterile PBS, weighed, and then homogenized with an Ultra Turrax blender (Ika-Werke, Staufen im Breisgau, Germany). Viable counts in homogenates were determined as described above. Data were analyzed by an analysis of variance followed by the Bonferroni posttest. Statistical significance was considered to be a P value of <0.05.

RNA extraction from infected tissues. Outbred 10-week-old female MF1 mice (Charles River) were intranasally infected as described above. When mice became severely lethargic, they were deeply anesthetized with 5% (vol/vol) isoflurane over oxygen, and blood was collected by cardiac puncture. Mice were killed by cervical dislocation, and the nasopharyngeal tissues were removed and homogenized on ice in 10 ml sterile PBS, using a tissue homogenizer as described above. To separate pneumococci from host cells, tissue homogenates and blood samples were centrifuged at 900 × *g* for 6 min at 4°C, as described previously (41). Supernatants were then centrifuged at 15,500 × *g* for 2 min at 4°C, and the bacterial pellet was stored at −80°C until further processing. Prior to pelleting, 20 μl of homogenate was removed, serially diluted in PBS, and plated onto blood agar in order to enumerate pneumococci and to exclude the presence of contaminating microflora. RNA was extracted by the TRIzol method, according to the manufacturer's instructions (Invitrogen, Paisley, United Kingdom). Briefly, the cell pellet was resuspended in 500 μl TRIzol reagent, vortexed for 15 s, and mixed thoroughly with 200 μl chloroform. The mixture was transferred into lysing matrix B tubes (MP Biomedicals, Cambridge, United Kingdom) that contained silica beads, and the cells were disrupted in a Ribolyser (Hybaid, Teddington, United Kingdom) for 45 s at a power setting of 6.5. The upper aqueous phase containing RNA was mixed with isopropanol, and RNA was pelleted by centrifugation at 12,000 × *g* for 10 min at 4°C. Finally, the pellet was washed with 70% (vol/vol) ethanol and dried at room temperature before being resuspended in DNase- and RNase-free water (Sigma). Any contaminating DNA was removed by treatment with 2 U RNase-free DNase I (Invitrogen) for 15 min at room temperature, followed by heat inactivation for 10 min at 65°C in the presence of 2.5 mM EDTA, and subsequently purified with an RNeasy minikit (Qiagen).

Statistical analysis. The significance of differences was determined by the unpaired t test. A P value of <0.05 was considered significant.

Ethics statement. Mouse experiments at the University of Leicester were performed under appropriate project (permit no. 80/2111) and personal (permit no. 80/10279) licenses according to the United Kingdom Home Office guidelines and local ethical approval. Where appropriate, the procedures were carried out under anesthetization with isoflurane. Mice were kept in individually ventilated cages in a controlled environment and were frequently monitored after infection, to minimize suffering.

The immunization of rabbits was performed at the Ben-Gurion University of the Negev under appropriate project (permit no. IL-46-10-2007) and personal (permit no. BGU-R-62-2006) licenses according to the guidelines of the National Council for Animal Research in Israel. Rabbits were housed under sterile conditions and were frequently monitored after immunizations, to minimize suffering.

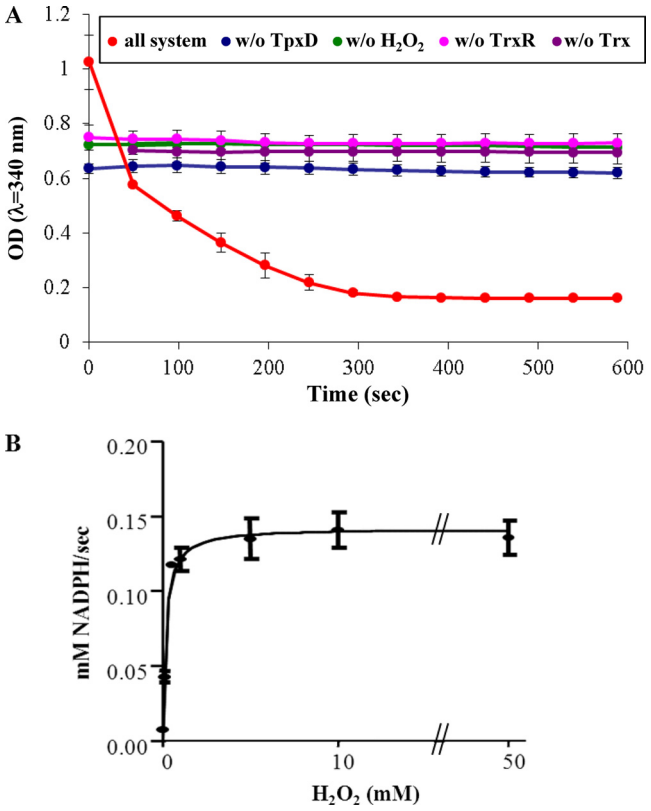

FIG 1 Peroxidase activity of recombinant TpxD using the thioredoxin system as a reductant. The reaction mixture contained 100 mM HEPES-NaOH (pH 7.0), 0.2 mM NADPH, 3.4 mM *E. coli* Trx, 0.36 mM *E. coli* TrxR, 5 μM purified TpxD, and 1 mM H_2O_2. Reactions were carried out with a total volume of 0.2 ml at 25°C and were started by the addition of H_2O_2 to the mixture. (A) Each curve is an absorbance time course at 340 nm, due to NADPH oxidation. In control experiments, TpxD (blue), H_2O_2 (green), thioredoxin reductase (pink), or thioredoxin (violet) was omitted from the reaction mixture. The data shown are from one representative experiment done in duplicates, but it was repeated 3 times, with similar results. (B) Michaelis-Menten curve for the determination of K_m, V_{max}, and K_{cat}/K_m values, with H_2O_2 concentrations plotted on the *x* axis and velocity plotted on the *y* axis.

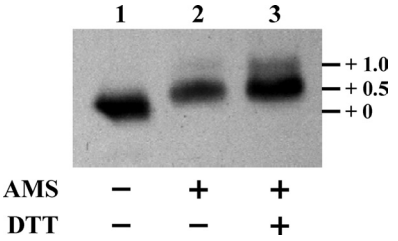

FIG 2 TpxD cysteine-thiol redox state under aerobic conditions. D39 cells were resuspended in AMS buffer supplemented with 20 mM AMS, sonicated, and incubated at room temperature for 2 h. Alkylated samples were loaded onto 18% (wt/vol) polyacrylamide–SDS gels and immunoblotted by using TpxD polyclonal antibodies. Reduced samples were prepared by incubating bacterial lysates with 50 mM DTT and then alkylated as described above. Lane 1, unalkylated lysates (no AMS added); lane 2, AMS-treated bacterial lysates; lane 3, lysates treated with DTT prior to AMS alkylation. Experiments were repeated 3 times.

RESULTS

NADPH-linked peroxidase activity of TpxD. In order to demonstrate that TpxD possess peroxidase activity, *S. pneumoniae* D39 TpxD was overexpressed in *E. coli* and purified to homogeneity. Figure 1A shows the peroxidase activity of TpxD, monitored by the decrease of the absorbance at 340 nm as NADPH becomes oxidized. In this assay system, TpxD uses H_2O_2 as a substrate, and an *E. coli* thioredoxin-thioredoxin reductase system transfers electrons from NADPH to TpxD (39). We found that recombinant TpxD catalyzed the reduction of H_2O_2 and that its activity was absolutely dependent on the presence of H_2O_2 and the thioredoxin-thioredoxin reductase recycling system. The rate of NADPH oxidation was plotted versus H_2O_2 concentrations (0.001 to 50 mM) and fitted to a Michaelis-Menten equation (Fig. 1B). The K_m and V_{max} values were calculated to be a K_m of 0.17 ± 0.04 mM, a V_{max} of 0.14 ± 0.01 mM/s, and a K_{cat}/K_m of $1.66 \pm 0.35 \times 10^5\ M^{-1}\ s^{-1}$, indicating that TpxD is able to reduce H_2O_2 efficiently.

TpxD redox state under aerobic conditions. TpxD catalytic activity in other bacteria was reported previously to require two conserved cysteine residues, which undergo specific oxidation for the reduction of H_2O_2 (22, 39). To check the pneumococcal TpxD oxidation state under aerobic conditions, TpxD cysteines in the reduced state were trapped with the high-molecular-mass (0.5 kDa) AMS moiety and then separated by SDS-PAGE. The results shown in Fig. 2 correspond to three different treatments: (i) untreated bacterial lysates (no AMS added), which simulate a state where all cysteine residues are oxidized and thus cannot bind AMS (Fig. 2, lane 1); (ii) AMS-treated lysates (Fig. 2, lane 2); and (iii) lysates treated with DTT prior to AMS alkylation (Fig. 2, lane 3). AMS treatment of wild-type strain D39, grown under aerobic conditions (Fig. 2, lane 2) resulted in two bands observed slightly above the unalkylated band in lane 1: a major lower band at +0.5 kDa, representing one cysteine residue in the reduced state (bound to an AMS molecule) and one cysteine in the oxidized state (no AMS bound), and a minor higher band at +1.0 kDa, representing two AMS-alkylated cysteines. This finding indicates that under aerobic conditions, most of the TpxD molecules contain one cysteine in the reduced state and one cysteine in the oxidized state. The fact that, under aerobic conditions, no band migrated fully oxidized (as observed for the unalkylated protein in lane 1) indicates that one of the cysteine residues is always in the reduced state, while the second cysteine can be either reduced or oxidized. DTT treatment of lysates prior to AMS alkylation (Fig. 2, lane 3) also yielded two bands at +0.5 and +1.0 kDa, indicating that only part of the oxidized cysteine residues were available for DTT reduction. However, the ratio of the intensities between the +0.5- and +1.0-kDa bands (measured by densitometry) was lower for the DTT-treated than for the untreated pneumococci.

To identify which cysteine was oxidized under aerobic conditions, D39 cells were treated with iodoacetate (IAA) to block cysteines that were still in the reduced state at harvesting, and homogenates were analyzed by SDS-PAGE. The TpxD band was cut from the gel, reduced, and then incubated with iodoacetamide (IAM) to label the cysteines that were oxidized during aerobic growth. Chymotrypsin digestion of the TpxD band that originated from aerobically grown D39 cells revealed the presence of the two cysteine residues in two separate peptides: (i) VLSVVPSIDTGIC^{58}STQTR and (ii) WC^{92}GAEGLDNAIMLSDYFDHSFGR. The first peptide was found in two variations—about half of the TpxD molecules presented Cys^{58} bound to IAA, i.e., in the reduced state, and half bound to IAM, i.e., in the oxidized state (see Fig. S1A in the supplemental material)—while the second peptide, containing Cys^{92},

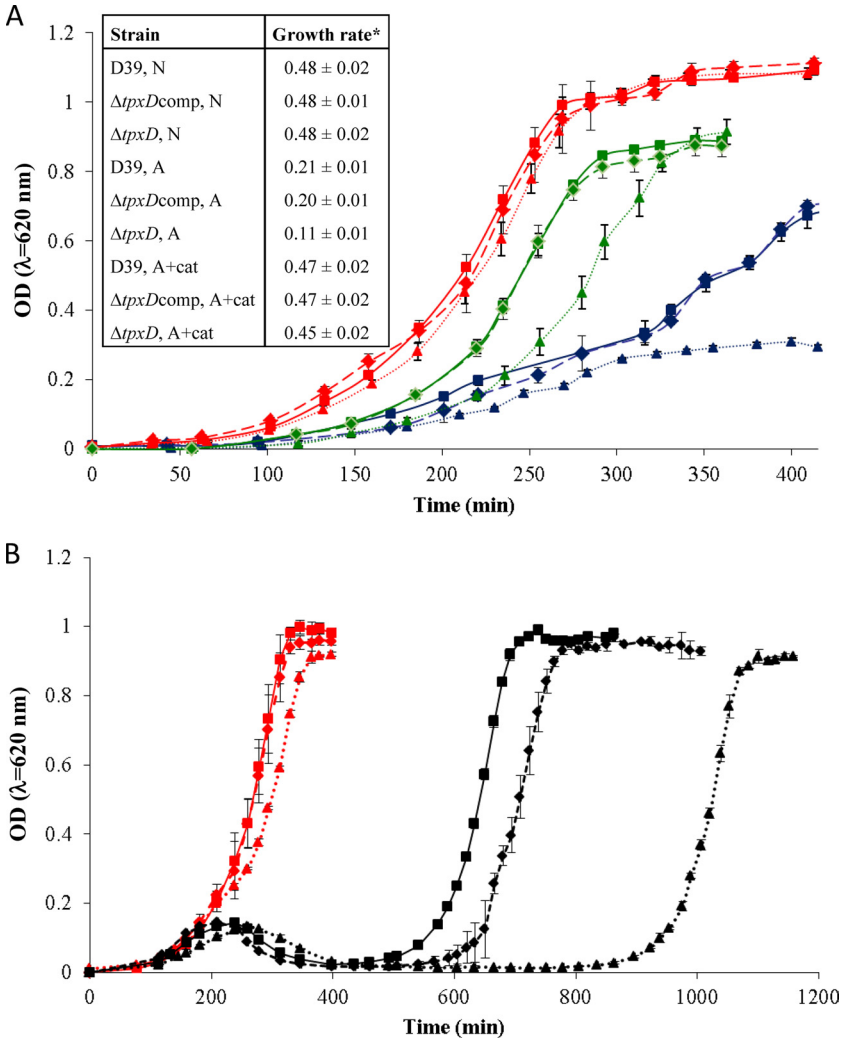

FIG 3 *tpxD* deletion impairs growth of D39 bacteria under aerobic conditions (A) and following a challenge with exogenous H_2O_2 (B). D39 (squares and solid lines), D39Δ*tpxD* (triangles and dotted lines), and D39Δ*tpxD*comp (diamonds and dashed lines) cells were grown in THY medium under anaerobic (N) conditions (red lines), aerobic conditions (A) (blue lines), and aerobic conditions in the presence of 1,000 U/ml catalase (A+cat) (green lines) (A) as well as under anaerobic conditions with (black lines) and without (red lines) the addition of 0.75 mM H_2O_2 (final concentration) at an OD_{620} of 0.05 (B). *, the growth rate is defined as the increase in OD_{620} units per hour. Values represent the means of data from at least 2 experiments in triplicates.

was always found to be bound to IAA, i.e., in the reduced state (see Fig. S1C in the supplemental material). In the DTT-treated lysates, the same two peptides were identified as in the aerobically grown D39 samples. However, most (~90%) of the Cys^{58} was reduced, and only a minor portion was oxidized (see Fig. S1B in the supplemental material). Here also, Cys^{92} was always found in the reduced state (see Fig. S1D in the supplemental material). These data indicate that Cys^{58} undergoes selective oxidation under aerobic conditions, suggesting its H_2O_2-scavenging activity.

Effect of the *tpxD* mutation on bacterial growth. The contribution of TpxD to *S. pneumoniae* growth in culture was checked by growing the wild-type D39 strain and its isogenic D39Δ*tpxD* mutant under aerobic and anaerobic conditions. Growth features were also determined for D39Δ*tpxD*comp, which was created by using plasmid pCEP containing the entire *tpxD* sequence plus a region of 83 bp upstream of the gene predicted to harbor the native promoter. Similar growth rates ($P > 0.05$) were measured for all 3 strains under anaerobic conditions (Fig. 3A). Under aerobic conditions, the 3 strains had an extended lag phase, a significantly reduced growth rate ($P < 0.005$), and lower maximal OD values than under anaerobic conditions. In addition, the growth rate of D39Δ*tpxD* under aerobic conditions was significantly lower than those of D39 and D39Δ*tpxD*comp ($P < 0.05$). This difference was eliminated when the strains were grown aerobically in the presence of the H_2O_2 scavenger catalase in the culture medium ($P > 0.05$), although the lag phase was still longer for D39Δ*tpxD* than for D39 and D39Δ*tpxD*comp, suggesting that in the lag phase, the residual endogenous H_2O_2, which is inaccessible to catalase, requires some adaptive response before growth. Hence, we suggest that TpxD is also important for the precise control of the H_2O_2 concentration in the lag phase. The difference observed in the lag phase was further studied by challenging lag-phase bacteria ($OD_{620} = 0.05$) grown under anaerobic conditions with exogenously added 0.75 mM H_2O_2 (Fig. 3B). This resulted in a remarkably extended lag phase in D39Δ*tpxD* cells compared to those of D39 and D39Δ*tpxD*comp cells, further supporting the

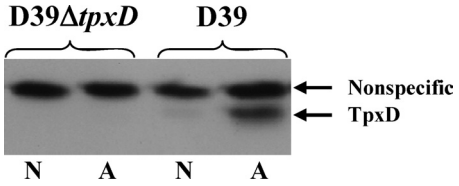

FIG 4 Increased TpxD synthesis under aerobic compared to anaerobic growth conditions. TpxD levels were measured in D39 and D39Δ*tpxD* cells grown to an OD_{620} of 0.3 in THY medium under aerobic (A) and anaerobic (N) conditions. Equal loading was validated by Ponceau staining of the nitrocellulose membrane and by the similar intensities of the nonspecific bands at about 21 kDa in the different lanes. Approximately 2.5×10^7 CFU from each sample were subjected to SDS-PAGE. The figure is a representative gel of 3 independent experiments.

conclusion that TpxD plays a crucial role against exogenous H_2O_2, especially during the lag phase.

TpxD improves pneumococcal survival upon challenge with exogenous H_2O_2. To further test the involvement of TpxD in the defense mechanism against oxidative stress, D39 and D39Δ*tpxD* mutant cells grown under aerobic conditions were challenged with exogenous H_2O_2 (see Fig. S2 in the supplemental material). Approximately 32% of D39 cells survived treatment with 40 mM H_2O_2, while only 8% of D39Δ*tpxD* cells survived this concentration ($P < 0.005$). The challenge of pneumococci with 20 mM H_2O_2 resulted in a 52% survival of D39 cells, versus 42% of D39Δ*tpxD* cells ($P < 0.005$). It is worth noting that no change in chain formation was observed between D39 and D39Δ*tpxD* bacteria and between H_2O_2-treated and untreated bacteria (data not shown).

Impaired H_2O_2 removal by D39Δ*tpxD*. We examined the concentration of H_2O_2 produced by batch cultures of 6×10^7 pneumococci per ml, incubated under aerobic conditions for 60 min, and found higher levels (about 20%) in the supernatants of D39Δ*tpxD* cells than in the supernatants of D39 cells: 936 ± 46 μM and 754 ± 64 μM ($n = 3$), respectively ($P < 0.001$). These results indicate that TpxD is able to detoxify a fraction of the H_2O_2 generated by the aerobic metabolism of the pneumococcus.

Increased levels of TpxD production under aerobic compared to anaerobic growth conditions. SDS-PAGE and Western blotting with anti-TpxD antibodies yielded two bands at about 18 and 21 kDa. Using mass spectrometry, we found that only the band at 18 kDa corresponded to pneumococcal TpxD (data not shown), while the upper band did not (i.e., a nonspecific band). Western blot data for D39 cells grown under aerobic compared to anaerobic conditions showed a strong TpxD band in cells grown under aerobic conditions, while under anaerobic conditions, a very weak band was visualized (Fig. 4). Transcript levels revealed the same trend: the *tpxD* transcription level was 5.8-fold ± 0.2-fold higher in D39 cells grown under aerobic conditions than under anaerobic conditions ($P < 0.001$).

Increased levels of *tpxD* expression and TpxD production following exposure to exogenous H_2O_2. To determine the dependence of TpxD synthesis and transcription on the H_2O_2 concentration (Fig. 5A to C) and time of exposure (Fig. 5D and E), D39 and D39Δ*tpxD*comp cells were grown anaerobically to an OD_{620} of 0.3 in THY medium and incubated for 40 min with 10 to 1,000 μM H_2O_2 (Fig. 5A to C). In addition, D39 cells were grown anaerobically to an OD_{620} of 0.3 in THY medium and exposed to 1,000 μM H_2O_2 for 2 to 60 min. Western blot analysis showed that

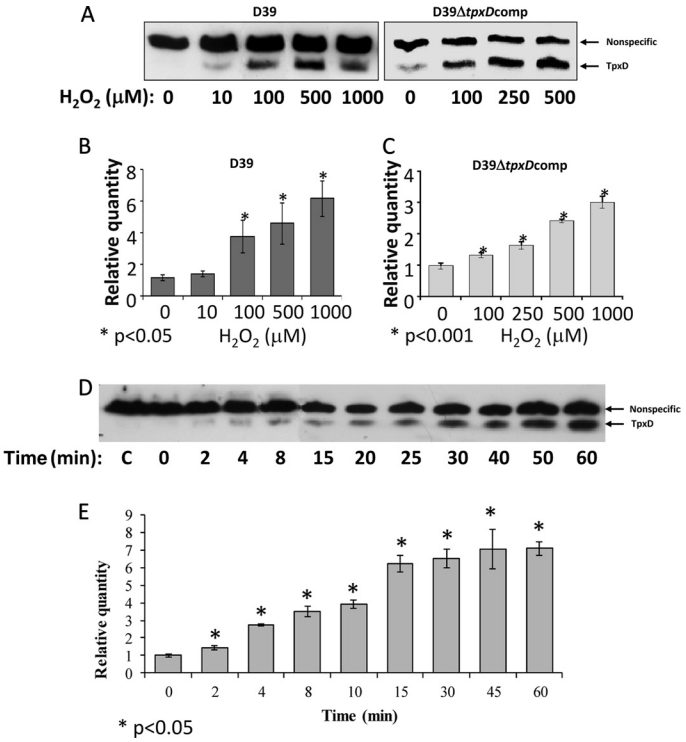

FIG 5 Increased levels of *tpxD* expression and TpxD production following exposure to exogenous H_2O_2. TpxD production levels determined by Western blotting (A and D) and *tpxD* expression levels determined by real-time RT-PCR (B, C, and E) were measured in D39 and D39Δ*tpxD*comp cells grown anaerobically to an OD_{620} of 0.3 in THY medium and then challenged with increasing H_2O_2 concentrations (10 to 1,000 μM) for 40 min (A to C) and in D39 cells challenged with 1,000 μM H_2O_2 for 2 to 60 min (D and E). C, control (D39 cells incubated with water [instead of H_2O_2] for 60 min). Values are representative of triplicate determinations for at least two independent experiments.

TpxD production was stimulated at an H_2O_2 concentration as low as 10 μM, and the intensity of the TpxD band increased with increasing H_2O_2 concentrations, reaching maximal intensity at approximately 100 μM H_2O_2 (Fig. 5A). Real-time RT-PCR results also showed increased *tpxD* transcription levels with increasing H_2O_2 concentrations ($P < 0.05$ for 100 to 1,000 μM) (Fig. 5B). Similar trends were also observed for D39Δ*tpxD*comp cells (Fig. 5A and C). The effect of H_2O_2 on *tpxD* expression was also examined for TIGR4: 500 μM H_2O_2 triggered an 11.8-fold ± 0.9-fold upregulation of *tpxD*.

To rule out the possibility that the plateau observed in Fig. 5A and B is due to cell death, the viability of D39 cells challenged with 1,000 μM H_2O_2 for 40 min was measured. It was found that even at this high concentration of H_2O_2, 90.7% of D39 cells remained viable.

D39 TpxD synthesis was very fast, with the 18-kDa TpxD band emerging within 2 min after the addition of 1,000 μM H_2O_2 (Fig. 5D), and reached maximal intensity after 30 min. As expected, *tpxD* transcript levels increased progressively ($P < 0.05$ for all time points versus the control), peaking at 15 min after exposure to 1,000 μM H_2O_2 (Fig. 5E).

The level of TpxD production decreases in the presence of catalase. To further establish the effect of exogenous H_2O_2 on *tpxD* expression, D39 cells were grown anaerobically and then

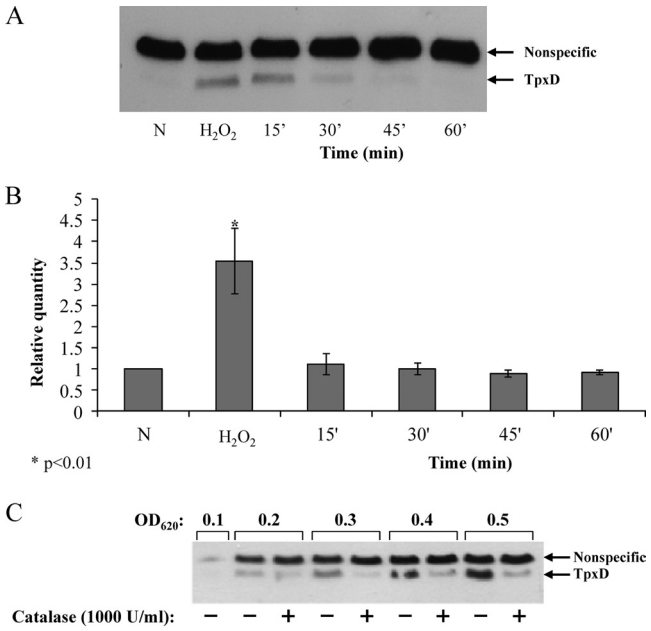

FIG 6 The level of TpxD production decreases in the presence of catalase. (A and B) The effects of exogenously added H_2O_2 on TpxD synthesis (A) and expression (B) were measured in D39 cells challenged with H_2O_2 (150 μM) for 30 min and then treated with catalase (12,000 U/ml) for the times indicated. Values are the means of data from duplicate determinations in two independent experiments and were normalized to the *tpxD* expression level in pneumococci grown anaerobically (N). (C) To evaluate the effect of endogenously produced H_2O_2 on TpxD synthesis, catalase (1,000 U/ml) was added to the culture medium of D39 cells grown aerobically each time the OD of the culture increased by 0.1 OD unit, beginning at an OD_{620} of 0.1. At each OD point, the TpxD level in catalase-treated bacterial cultures was determined and compared to that in the untreated culture.

treated with H_2O_2 (150 μM) for 15 min. Subsequently, catalase (12,000 units/ml) was added to the culture medium to ensure the complete scavenging of H_2O_2. As shown in Fig. 6A, TpxD synthesis was induced following the addition of H_2O_2 to the culture medium. Furthermore, H_2O_2 removal by catalase resulted in a time-dependent drop in the intensity of the TpxD band (Fig. 6A). The expression level of *tpxD* was also reduced following catalase treatment (Fig. 6B).

The effect of endogenous H_2O_2 produced by *S. pneumoniae* on TpxD synthesis was verified by measuring TpxD levels of catalase-treated, aerobically grown bacteria; catalase (1,000 units/ml) was added to the culture medium each time the OD of the culture increased by 0.1 OD units, beginning at an OD_{620} of 0.1. For example, catalase was added four times to pneumococcal cultures that were harvested at an OD_{620} of 0.5. At each 0.1 OD point, the TpxD level was tested in the catalase-treated culture and compared to that of the untreated culture. As shown in Fig. 6C, the addition of catalase resulted in a dramatic reduction in the level of TpxD synthesis. These data establish that H_2O_2, whether exogenously added or endogenously produced, determines the level of TpxD.

***tpxD* expression is coregulated with the *psa*-manganese transporter.** It was shown previously that the PsaBCA-manganese transport system and TpxD are involved in pneumococcal resistance to oxidative stress (26, 42). To check whether the *psa* operon is affected by *tpxD*, we measured the expression levels of *psaBCA* in D39Δ*tpxD* cells compared to those in D39 cells under anaerobic conditions and found that the genes encoding the Mn^{2+} transport system were significantly downregulated in the D39Δ*tpxD* mutant ($P < 0.001$) (Fig. 7A), indicating that TpxD is involved in the regulation of *psaBCA*. Further characterization of this regulation came from the observation that *psaBCA* expression levels in D39 cells grown under aerobic conditions were about half of the levels under anaerobic conditions. However, similar levels were measured for D39Δ*tpxD* cells grown under aerobic and anaerobic conditions (Fig. 7A).

The effect of H_2O_2 on *psaBCA* expression levels was tested by challenging bacteria with H_2O_2 (100 to 1,000 μM). Our data show that H_2O_2 triggered the downregulation of *psaBCA* in D39 ($P < 0.001$) but had no effect on D39Δ*tpxD* (Fig. 7B), suggesting that the coregulation of *tpxD* and *psaBCA* is controlled by H_2O_2 and TpxD. To eliminate the possibility that the downregulation of *psaBCA* originated from polar effects of the *tpxD* mutation, experiments were repeated with D39Δ*tpxD*comp cells. As shown in Fig. 7C, *tpxD* complementation restored the effect of H_2O_2 on *psaBCA*. The effect of TpxD on *psaBCA* expression was also tested in a TIGR4 background: as for D39 cells, *psaBCA* were downregulated following a challenge with 500 μM H_2O_2, and similar *psaBCA* levels were measured in TIGR4Δ*tpxD* cells challenged with H_2O_2 compared to the unchallenged mutant strain (Fig. 7D).

Impaired virulence of D39Δ*tpxD* in intranasally infected mice. The contribution of TpxD to pneumococcal virulence and survival in different host tissues was determined in a mouse model of pneumococcal infection. The median survival time of mice infected intranasally with D39Δ*tpxD* was significantly longer ($P < 0.01$) than those of the D39- and D39Δ*tpxD*comp-infected cohorts (75 versus 48 and 42 h, respectively) (Fig. 8A). However, when bacteria were administered directly into blood, where the oxygen tension is low relative to that in the nasopharynx, the difference in the median survival time between D39Δ*tpxD*, the wild-type strain, and D39Δ*tpxD*comp disappeared (56, 56, and 68 h, respectively) ($P > 0.05$) (Fig. 8B). The impaired virulence of D39Δ*tpxD* was further investigated by determining the growth of pneumococci in the nasopharynx (Fig. 9A) and in the blood (Fig. 9B) following intranasal infection. The numbers of D39Δ*tpxD* bacteria in the nasopharynx were significantly smaller than the numbers of the wild type and D39Δ*tpxD*comp at 12 h postinfection ($P < 0.001$) (Fig. 9A). However, from this point onward, the numbers of mutant bacteria increased and were not significantly different from those of the wild type at 24 h postinfection ($P > 0.05$). Bacteremia could be detected 12 h after intranasal infection in all three infected cohorts, yet at 24 and 36 h postinfection, the numbers of D39Δ*tpxD* bacteria in blood were significantly smaller than those of the wild-type strain and D39Δ*tpxD*comp ($P < 0.05$ and $P < 0.01$ at 24 and 36 h postinfection, respectively) (Fig. 9B). There was no difference in growth between the wild type and D39Δ*tpxD*comp in blood or in the nasopharynx ($P > 0.05$), indicating that the observed *in vivo* attenuation in growth is due to the *tpxD* deletion rather than a polar effect of the *tpxD* mutation.

***In vivo* expression of *tpxD* and *psaBCA*.** The expression levels of *psaBCA* and *tpxD* were determined for D39 cells recovered from the nasopharynx and blood following intranasal infection. Real-time RT-PCR data (Fig. 10) revealed that *tpxD* was downregulated in the less aerated niche of the blood compared to the nasopharynx, whereas *psaBCA* were upregulated. These results show that while *tpxD* expression is induced in oxygenated tissue

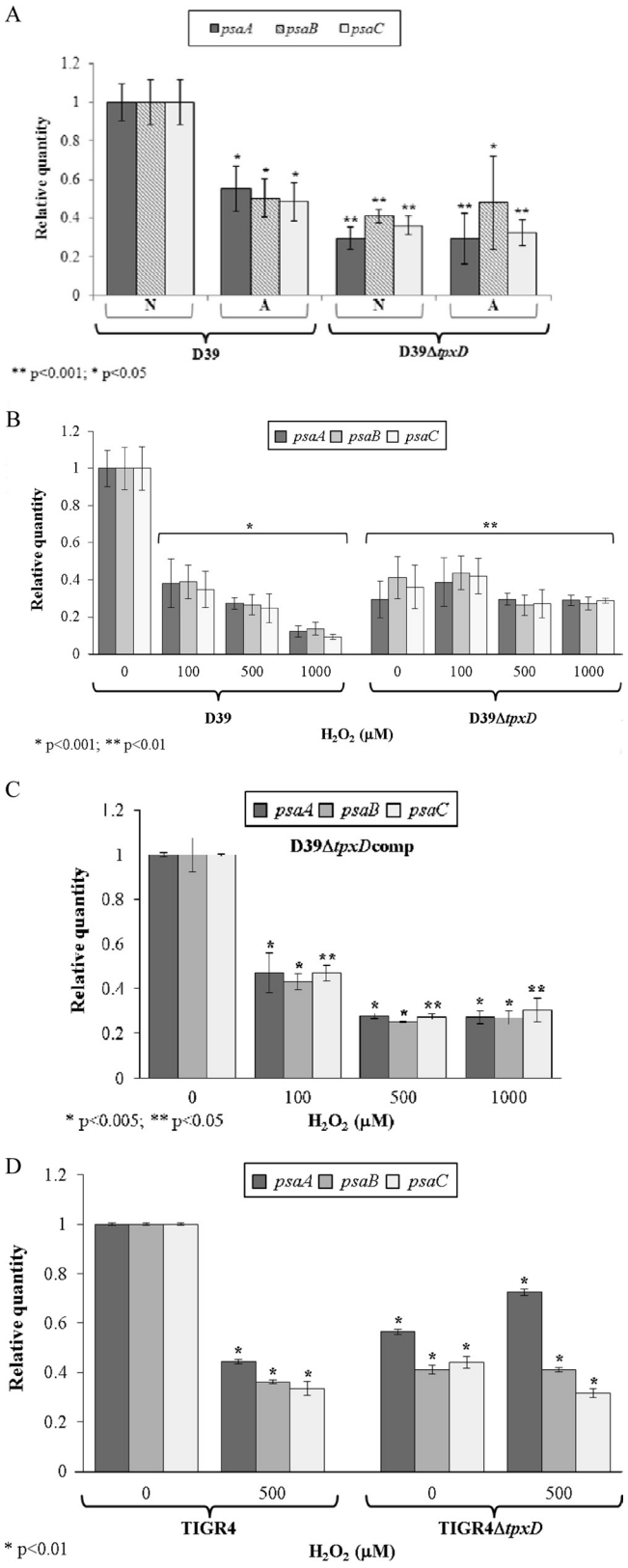

FIG 7 Coregulation of *psaBCA* and *tpxD in vitro*. Expression levels of *psaBCA* were measured in D39 and D39Δ*tpxD* cells grown under aerobic and anaerobic conditions (A), D39 and D39Δ*tpxD* cells challenged for 40 min with 100 to 1,000 μM H_2O_2 (B), D39Δ*tpxD*comp cells challenged for 40 min with 100 to 1,000 μM H_2O_2 (C), and TIGR4 and TIGR4Δ*tpxD* cells challenged for 40 min with 500 μM H_2O_2 (D). Results are expressed as relative quantities, where *tpxD* levels in wild-type bacteria grown under anaerobic conditions were normalized to 1. Values are the means of data from duplicate determinations in at least 2 independent experiments. A, aerobic conditions; N, anaerobic conditions. *P* values were calculated relative to *tpxD* levels in wild-type bacteria grown under anaerobic conditions.

sites, the expression levels of *psaBCA* are repressed, correlating with the *in vitro* effect of the H_2O_2 challenge (Fig. 5 and 7).

DISCUSSION

Streptococcus pneumoniae is a facultative anaerobic pathogen. Although it maintains a fermentative metabolism, during growth in air, *S. pneumoniae* produces high levels of H_2O_2 (34), which can have adverse effects on cell viability and DNA (15, 16). As this organism lacks proteins that have been shown to protect against oxidative stress (e.g., catalase) (10), several studies focused on pneumococcal H_2O_2 resistance (34, 37, 42). This resistance is important not only for the oxidative stress response of the pathogen but also for pneumococcal physiology (7, 36) and pneumococcal interactions with other bacteria (24, 33, 40) and the host (12, 13, 35). Although it had been speculated that *tpxD* (*psaD*) encodes a pneumococcal thiol peroxidase, this is the first report that established the identity of the protein by direct enzymatic assays, demonstrated its mechanism of action, and showed that TpxD expression is regulated in response to H_2O_2 levels. Furthermore, this is the first demonstration of the coordinated expression of *tpxD* and the three other *psaBCA* genes in the *psa* operon of *S. pneumoniae*.

As the first step toward an understanding the enzymatic activity of TpxD, we measured the thiol peroxidase activity of a recombinant TpxD protein toward H_2O_2, using a proposed physiological electron donor system, thioredoxin plus thioredoxin reductase, linked to NADPH oxidation (4, 5). Our results showed that the recombinant pneumococcal TpxD protein had a relatively high level of peroxidase activity, similar to those obtained for *E. coli* (4) and *Helicobacter pylori* (5). The oxidation of NADPH was not observed in the absence of either TpxD or H_2O_2, thioredoxin, and thioredoxin reductase, indicating that pneumococcal TpxD is a thioredoxin-dependent peroxidase.

The scavenging of H_2O_2 by thiol peroxidase requires the specific oxidation of the peroxidatic cysteine, which in turn oxidizes a second (resolving) cysteine, to produce a disulfide bond (39). We used mass spectrometry and a thiol-trapping method to determine the redox states of the two predicted catalytic cysteine residues of TpxD under aerobic conditions (TpxD could hardly be detected by Western blotting under anaerobic conditions). Our data show that most of the TpxD molecules had the peroxidatic cysteine (Cys^{58}) in the oxidized state, while the resolving cysteine (Cys^{92}) was always found in the reduced state. In the DTT-treated lysates, a larger portion of the Cys^{58} residues were reduced. The fact that DTT was unable to reduce all the peroxidatic cysteine residues can be explained by an irreversible overoxidation of Cys^{58} during TpxD turnover, a phenomenon previously described for *E. coli* Tpx (4). We could not detect the resolving cysteine in the oxidized form, and we speculate that the disulfide bond between Cys^{92} and Cys^{58} undergoes a quick reduction by a thioredoxin system to make it available for the next scavenging cycle.

Strain D39Δ*tpxD* was viable under aerobic conditions but grew

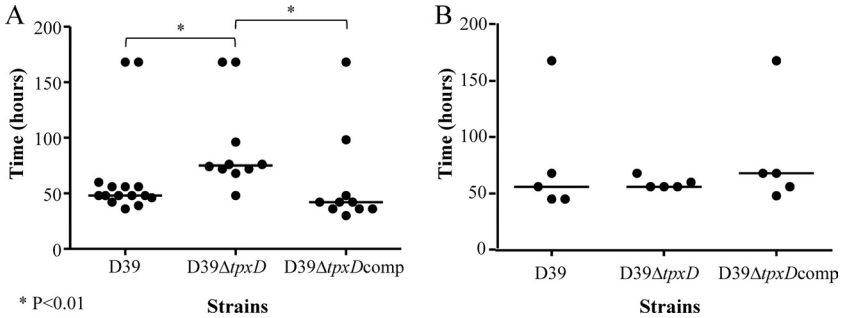

FIG 8 Impaired virulence of D39Δ*tpxD* cells following intranasal infection. Mice were infected intranasally with approximately 1×10^6 CFU (A) or intravenously with approximately 5×10^5 CFU (B) of either D39, D39Δ*tpxD*, or D39Δ*tpxD*comp. The animals were monitored over 168 h. Symbols show the times when individual mice became severely lethargic, the point when the animals were culled. The horizontal bars mark the median times to the severely lethargic state.

more slowly than the wild type. The difference in growth rates disappeared when bacteria were grown under anaerobic conditions. When bacteria were grown under aerobic conditions in the presence of an H_2O_2 scavenger, catalase, the growth rates were still the same, but the duration of the lag phase of D39Δ*tpxD* was significantly longer than that of D39, implying that TpxD is important for the precise control of the H_2O_2 concentration produced by the organism in the lag phase, in addition to its role in the log phase. D39Δ*tpxD* was also more susceptible to exogenous H_2O_2 challenge than the wild-type strain, in agreement with data from previous reports (26, 42). Further support for the role of TpxD in H_2O_2 resistance came from the observation that levels of *tpxD* expression and synthesis were significantly increased in pneumococci grown under aerobic compared to anaerobic conditions and in the presence of exogenously added H_2O_2. In addition, the removal of H_2O_2 by catalase resulted in a drop in the levels of *tpxD* expression and synthesis. Furthermore, a higher level of *tpxD* transcription *in vivo* was observed in a highly aerated niche of infected mice, i.e., the nasopharynx, than in the less aerated niche of the blood. These data show that *tpxD* transcription and synthesis are modulated, both *in vivo* and *in vitro*, in response to H_2O_2 levels. This conclusion is supported by a previous report by Ramos-Montanez et al., who showed that the relative amounts of *tpxD* transcripts decreased approximately 2-fold in a Δ*spxB* mutant that is defective in H_2O_2 production (38). Interestingly, Tpx proteins from *Campylobacter jejuni* and *E. coli* are induced by molecular oxygen rather than H_2O_2 (2).

The *tpxD* gene is located downstream of the *psaBCA* genes, coding for an ABC Mn^{2+}-permease complex. It is believed that there is a significant readthrough from the *psa* promoter to *tpxD*, although *tpxD* has its own promoter (29). Hence, we looked at the interrelation between the expression levels of *psaBCA* and those of *tpxD* and found that *psaBCA* were downregulated under aerobic compared to anaerobic conditions and in response to H_2O_2 challenges with both D39 and TIGR4, notwithstanding the increase in the *tpxD* expression level, suggesting that the expressions of *psaBCA* and *tpxD* are under the control of different promoters. Furthermore, no change in *psaBCA* expression levels was measured for both D39Δ*tpxD* and TIGR4Δ*tpxD* cells challenged with H_2O_2. These data suggest that TpxD is involved in the regulation of the *psa* operon as part of the bacterial response to oxidative stress conditions. Of note is the finding that the genes encoding the Mn^{2+} transport system were significantly downregulated under anaerobic conditions in D39Δ*tpxD* bacteria compared to wild-type bacteria, implying that TpxD is involved in the regulation of *psaBCA* even in the absence of H_2O_2.

The coregulation of *psaBCA* and *tpxD* was further established *in vivo* by comparing the expression levels in two niches of infected mice, which differ in oxygen tension. Our data show an inverse correlation of the expression levels of *psaBCA* and *tpxD* *in vivo*, i.e., increased *psaBCA* and decreased *tpxD* levels in the blood compared to the highly aerated niche of the nasopharynx, in agreement with the *in vitro* expression levels in wild-type cells grown under aerobic versus anaerobic conditions or challenged with

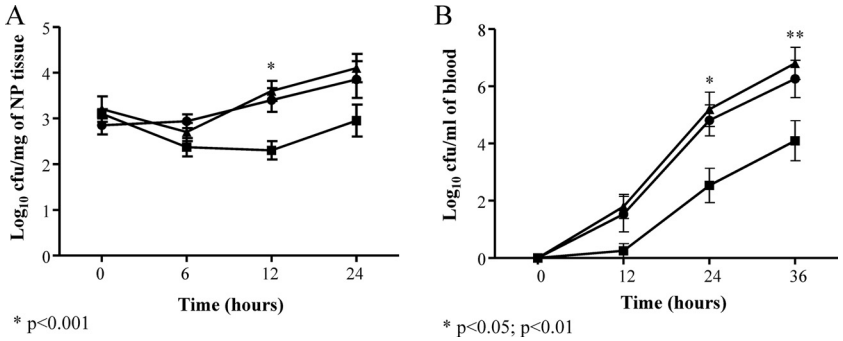

FIG 9 Impaired growth of D39Δ*tpxD* cells (■) compared to D39 (●) and D39Δ*tpxD*comp (▲) cells in the nasopharynx (NP) (A) and the blood (B). The growth of each strain was determined in infected tissues up to 36 h after intranasal infection with approximately 1×10^6 bacteria. A sample of blood taken from the tail vein or homogenized nasopharyngeal tissues were serially diluted, and the bacterial counts were determined by plating serial dilutions onto blood agar plates. Each point is the mean of data from five mice. Error bars show the standard errors of the means.

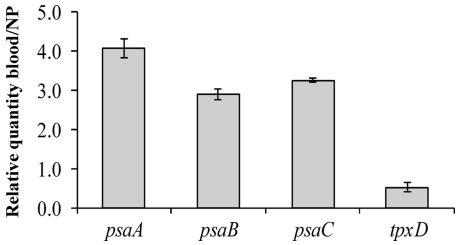

FIG 10 Coregulation of *psaBCA* and *tpxD in vivo*. *tpxD* and *psaBCA* expression levels were measured in tissues isolated from the nasopharynx (NP) and blood of D39-infected mice. Results are expressed as relative quantities after normalizing the expression level of each gene to that of *gyrA* and are represented as blood/NP. Results represent the means and standard deviations of data from three independent experiments.

H_2O_2. However, *in vivo* data reported previously by Mahdi et al. (23) showed higher *psaA* levels for D39 in the nose than in blood, while LeMessurier et al. (20) stated that *psaA* did not show a consistent difference in expression levels between those niches. It was shown previously that intracellular Mn^{2+} negatively affects the transcription of *psaBCA* (17). Since Mn^{2+} concentrations vary among the different niches in which *S. pneumoniae* resides within the host, i.e., higher Mn^{2+} concentrations in the nasopharynx than in the blood (31), it seems more likely that *psaA* levels will be downregulated in the nose, which contains higher manganese levels, in accordance with the data presented in this study. Mn^{2+} is known to be important for detoxifying superoxide and H_2O_2 (14). The inverse regulation of *psaBCA* and *tpxD* may imply that because of the competing requirements of some systems in different niches, such as Mn^{2+} uptake, the pneumococcus uses different oxidative defense mechanisms.

Mutant strain D39Δ*tpxD* was less virulent than the wild-type strain, as assessed by the survival times of intranasally infected mice, and it showed a significant decrease in its ability to survive in the nasopharynx during early stages of infection. Further support for this observation came from the *in vitro* growth curves, which showed a significantly longer lag phase in D39Δ*tpxD* than in D39 cells following a challenge with H_2O_2. Moreover, there were notable differences in D39Δ*tpxD* cell numbers relative to those of D39 in the blood following nasopharyngeal infection. However, when D39Δ*tpxD* was administered intravenously, it was as virulent as the wild type. These results are consistent with the conclusion that the growth attenuation of D39Δ*tpxD* following intranasal infection is due to an impaired ability of the mutant to deal with oxygen by-products in respiratory tissues. However, one cannot exclude the possibility that the attenuated virulence of the D39Δ*tpxD* mutant originates from the decreased expression levels of *psaBCA* (as measured by our *in vitro* system), since PsaBCA can also affect the sensitivity of *S. pneumoniae* to oxidative stress (26).

The *tpxD* gene was reported previously to be part of the core pneumococcal genome (30), indicating the importance of balancing the H_2O_2 concentration for the bacterium. Our data on the survival of intravenously infected mice are in agreement with findings by McAllister et al., who reported no significant difference in the median survival times of BALB/c mice challenged intraperitoneally with the Δ*tpxD* mutant and D39 (26). In contrast, Berry and Paton reported previously that mice infected with D39Δ*tpxD* survived significantly longer than the wild-type-infected cohort following an intraperitoneal infection with 3×10^3 CFU (8). Furthermore, those researchers were unable to show any difference in the median survival times between the wild-type- and D39Δ*tpxD*-infected groups following nasopharyngeal infection. While McAllister et al. did not test the contribution of TpxD in survival experiments following intranasal challenge, they reported no significant difference in the recoveries of wild-type and D39Δ*tpxD* bacteria from the nasopharynx of CD-1 mice with an infection dose of 4×10^6 to 2×10^7 CFU, in contrast to data presented in this study. The notably higher inoculum used by McAllister et al. could have overridden the effect of the mutation. In addition, other reasons may also account for the differences, including the preparation of the infective dose, the route of infection, and the mouse strain. One noteworthy feature of this study is that we passaged pneumococci to standardize the inoculum, whereas those other studies used bacteria solely grown *in vitro* for infection (8, 26), a practice which can result in variations of the *in vivo* phenotype.

The findings of this study confirm that *S. pneumoniae tpxD* encodes a functional thiol peroxidase involved in the scavenging of H_2O_2 and that TpxD synthesis is modulated, both *in vitro* and *in vivo*, in response to H_2O_2. Hence, higher levels of H_2O_2 accumulated in the culture supernatant of D39Δ*tpxD* bacteria than in the culture supernatant of wild-type bacteria. However, even in the wild type, which contains a functional TpxD protein, the level of H_2O_2 was quite high, suggesting that TpxD detoxifies only a fraction of the H_2O_2 generated by the pneumococcus under aerobic conditions, to maintain homeostatic levels of H_2O_2. In addition, our data demonstrate that the effect of H_2O_2 on *psaBCA* expression is mediated by TpxD. This may constitute one of the components of the organism's fundamental strategy to fine-tune cellular processes in response to H_2O_2. The links between the expressions of *tpxD* and *psaBCA* will be examined further by transcript mapping of bacteria challenged with H_2O_2.

ACKNOWLEDGMENTS

We thank the Smoler Proteomics Center at Technion, Israel, for mass spectrometry analysis.

This work was partially supported by grant 5110 from the Ministry of Health, Israel.

REFERENCES

1. **Alloing G, Granadel C, Morrison DA, Claverys JP.** 1996. Competence pheromone, oligopeptide permease, and induction of competence in *Streptococcus pneumoniae.* Mol. Microbiol. **21**:471–478.
2. **Atack JM, Harvey P, Jones MA, Kelly DJ.** 2008. The *Campylobacter jejuni* thiol peroxidases Tpx and Bcp both contribute to aerotolerance and peroxide-mediated stress resistance but have distinct substrate specificities. J. Bacteriol. **190**:5279–5290.
3. **Auzat I, et al.** 1999. The NADH oxidase of *Streptococcus pneumoniae*: its involvement in competence and virulence. Mol. Microbiol. **34**:1018–1028.
4. **Baker L, Poole LB.** 2003. Catalytic mechanism of thiol peroxidase from *Escherichia coli.* J. Biol. Chem. **278**:9203–9211.
5. **Baker LMS, Raudonikiene A, Hoffman PS, Poole LB.** 2001. Essential thioredoxin-dependent peroxiredoxin system from *Helicobacter pylori*: genetic and kinetic characterization. J. Bacteriol. **183**:1961–1973.
6. **Beer I, Barnea E, Ziv T, Admon A.** 2004. Improving large-scale proteomics by clustering of mass spectrometry data. Proteomics **4**:950–960.
7. **Benisty R, Cohen AY, Feldman A, Cohen Z, Porat N.** 2010. Endogenous H_2O_2 produced by *Streptococcus pneumoniae* control FabF activity. Biochim. Biophys. Acta **1801**:1098–1104.
8. **Berry AM, Paton JC.** 1996. Sequence heterogeneity of PsaA, a 37-kilodalton putative adhesin essential for virulence of *Streptococcus pneumoniae.* Infect. Immun. **64**:5255–5262.

9. **Bersani NA, Merwin JR, Lopez NI, Pearson GD, Merrill GF.** 2002. Protein electrophoretic mobility shift assay to monitor redox state of thioredoxin in cells. Methods Enzymol. **347**:317–326.
10. **Chapuy-Regaud S, et al.** 2001. Competence regulation by oxygen availability and by Nox is not related to specific adjustment of central metabolism in *Streptococcus pneumoniae.* J. Bacteriol. **183**:2957–2962.
11. **Guiral S, et al.** 2006. Construction and evaluation of a chromosomal expression platform (CEP) for ectopic, maltose-driven gene expression in *Streptococcus pneumoniae.* Microbiology **152**:343–349.
12. **Hirst RA, et al.** 2000. Relative roles of pneumolysin and hydrogen peroxide from *Streptococcus pneumoniae* in inhibition of ependymal ciliary beat frequency. Infect. Immun. **68**:1557–1562.
13. **Hoffmann O, et al.** 2006. Interplay of pneumococcal hydrogen peroxide and host-derived nitric oxide. Infect. Immun. **74**:5058–5066.
14. **Horsburgh MJ, Wharton SJ, Karavolos M, Foster SJ.** 2002. Manganese: elemental defence for a life with oxygen. Trends Microbiol. **10**:496–501.
15. **Imlay JA, Chin SM, Linn S.** 1988. Toxic DNA damage by hydrogen peroxide through the Fenton reaction *in vivo* and *in vitro.* Science **240**: 640–642.
16. **Imlay JA, Linn S.** 1986. Bimodal pattern of killing of DNA-repair-defective or anoxically grown *Escherichia coli* by hydrogen peroxide. J. Bacteriol. **166**:519–527.
17. **Johnston JW, Briles DE, Myers LE, Hollingshead SK.** 2006. Mn2-dependent regulation of multiple genes in *Streptococcus pneumoniae* through PsaR and the resultant impact on virulence. Infect. Immun. **74**: 1171–1180.
18. **Kadioglu A, Weiser JN, Paton JC, Andrew PW.** 2008. The role of *Streptococcus pneumoniae* virulence factors in host respiratory colonization and disease. Nat. Rev. Microbiol. **6**:288–301.
19. **Lampe DJ, Churchill ME, Robertson HM.** 1996. A purified mariner transposase is sufficient to mediate transposition *in vitro.* EMBO J. **15**: 5470–5479.
20. **LeMessurier KS, Ogunniyi AD, Paton JC.** 2006. Differential expression of key pneumococcal virulence genes *in vivo.* Microbiology **152**:305–311.
21. **Livak KJ, Schmittgen TD.** 2001. Analysis of relative gene expression data using real-time quantitative PCR and the $2^{(-\Delta\Delta C_T)}$ method. Methods **25**: 402–408.
22. **Lu J, et al.** 2008. Reversible conformational switch revealed by the redox structures of *Bacillus subtilis* thiol peroxidase. Biochem. Biophys. Res. Commun. **373**:414–418.
23. **Mahdi LK, Ogunniyi AD, LeMessurier KS, Paton JC.** 2008. Pneumococcal virulence gene expression and host cytokine profiles during pathogenesis of invasive disease. Infect. Immun. **76**:646–657.
24. **Margolis E.** 2009. Hydrogen peroxide-mediated interference competition by *Streptococcus pneumoniae* has no significant effect on *Staphylococcus aureus* nasal colonization of neonatal rats. J. Bacteriol. **191**:571–575.
25. **Martin B, Prudhomme M, Alloing G, Granadel C, Claverys JP.** 2000. Cross-regulation of competence pheromone production and export in the early control of transformation in *Streptococcus pneumoniae.* Mol. Microbiol. **38**:867–878.
26. **McAllister LJ, et al.** 2004. Molecular analysis of the psa permease complex of *Streptococcus pneumoniae.* Mol. Microbiol. **53**:889–901.
27. **McCluskey J, Hinds J, Husain S, Witney A, Mitchell T.** 2004. A two-component system that controls the expression of pneumococcal surface antigen A (PsaA) and regulates virulence and resistance to oxidative stress in *Streptococcus pneumoniae.* Mol. Microbiol. **51**:1661–1675.
28. **Morton DB.** 1985. Pain and laboratory animals. Nature **317**:106. doi: 10.1038/317106a0.
29. **Novak R, Braun JS, Charpentier E, Tuomanen E.** 1998. Penicillin tolerance genes of *Streptococcus pneumoniae*: the ABC-type manganese permease complex Psa. Mol. Microbiol. **29**:1285–1296.
30. **Obert C, et al.** 2006. Identification of a candidate *Streptococcus pneumoniae* core genome and regions of diversity correlated with invasive pneumococcal disease. Infect. Immun. **74**:4766–4777.
31. **Ogunniyi AD, et al.** 2010. Central role of manganese in regulation of stress responses, physiology, and metabolism in *Streptococcus pneumoniae.* J. Bacteriol. **192**:4489–4497.
32. **Paterson GK, Blue CE, Mitchell TJ.** 2006. An operon in *Streptococcus pneumoniae* containing a putative alkylhydroperoxidase D homologue contributes to virulence and the response to oxidative stress. Microb. Pathog. **40**:152–160.
33. **Pericone CD, Overweg K, Hermans PWM, Weiser JN.** 2000. Inhibitory and bactericidal effects of hydrogen peroxide production by *Streptococcus pneumoniae* on other inhabitants of the upper respiratory tract. Infect. Immun. **68**:3990–3997.
34. **Pericone CD, Park S, Imlay JA, Weiser JN.** 2003. Factors contributing to hydrogen peroxide resistance in *Streptococcus pneumoniae* include pyruvate oxidase (SpxB) and avoidance of the toxic effects of the Fenton reaction. J. Bacteriol. **185**:6815–6825.
35. **Perry F, Elson C, Greenham L, Catterall J.** 1993. Interference with the oxidative response of neutrophils by *Streptococcus pneumoniae.* Thorax **48**:364–369.
36. **Potter AJ, Kidd SP, McEwan AG, Paton JC.** 2010. The MerR/NmlR family transcription factor of *Streptococcus pneumoniae* responds to carbonyl stress and modulates hydrogen peroxide production. J. Bacteriol. **192**:4063–4066.
37. **Pulliainen AT, Haataja S, Kähkönen S, Finne J.** 2003. Molecular basis of H_2O_2 resistance mediated by streptococcal Dpr. J. Biol. Chem. **278**:7996–8005.
38. **Ramos-Montanez S, et al.** 2008. Polymorphism and regulation of the *spxB* (pyruvate oxidase) virulence factor gene by a CBS-HotDog domain protein (SpxR) in serotype 2 *Streptococcus pneumoniae.* Mol. Microbiol. **67**:729–746.
39. **Rho B, et al.** 2006. Functional and structural characterization of a thiol peroxidase from *Mycobacterium tuberculosis.* J. Mol. Biol. **361**:850–863.
40. **Selva L, Viana D, Regev-Yochay G, Trzcinski K, Corpa JM.** 2009. Killing niche competitors by remote-control bacteriophage induction. Proc. Natl. Acad. Sci. U. S. A. **106**:1234–1238.
41. **Terra VS, Homer KA, Rao SG, Andrew PW, Yesilkaya H.** 2010. Characterization of novel beta-galactosidase activity that contributes to glycoprotein degradation and virulence in *Streptococcus pneumoniae.* Infect. Immun. **78**:348–357.
42. **Tseng HJ, McEwan AG, Paton JC, Jennings MP.** 2002. Virulence of *Streptococcus pneumoniae*: PsaA mutants are hypersensitive to oxidative stress. Infect. Immun. **70**:1635–1639.
43. **Wan XY, et al.** 1997. Scavengase p20: a novel family of bacterial antioxidant enzymes. FEBS Lett. **407**:32–36.
44. **Woo H, et al.** 2003. Reversing the inactivation of peroxiredoxins caused by cysteine sulfinic acid formation. Science **300**:653–656.
45. **Yesilkaya H, et al.** 2000. Role of manganese-containing superoxide dismutase in oxidative stress and virulence of *Streptococcus pneumoniae.* Infect. Immun. **68**:2819–2826.
46. **Yesilkaya H, Manco S, Kadioglu A, Terra VS, Andrew PW.** 2008. The ability to utilize mucin affects the regulation of virulence gene expression in *Streptococcus pneumoniae.* FEMS Microbiol. Lett. **278**:231–235.
47. **Yesilkaya H, et al.** 2009. Pyruvate formate lyase is required for pneumococcal fermentative metabolism and virulence. Infect. Immun. **77**:5418–5427.